Hybrid Event-Triggered Low-Computation Adaptive Control for Switched Nonlinear Systems with Unmeasurable States

Tiantian Teng, Nannan Zhao and Xinyu Ouyang

Abstract—**Aiming at the problem of switched nonlinear system control with limited communication resources, a dual-channel output-feedback tracking control method with output and control event-triggered is designed in this paper. Firstly, the output signal is sampled by an output-based trigger detector, which is then integrated into state observers to estimate unknown states. Subsequently, in conjunction with Barrier Lyapunov Functions (BLFs) and the observer's results, the issue of non-differentiable virtual control laws post-sampling is solved, while the tracking and state errors are constrained. Additionally, the control event-triggering mechanism and the mismatch between switching and triggering intervals are also considered. The stability of each subsystem and the entire system under average dwell time is demonstrated by Lyapunov stability theory, along with boundedness of all signals. Finally, numerical simulation experiments verify the effectiveness of the proposed scheme.**

Index Terms—**Switched nonlinear systems, Output-feedback, Barrier Lyapunov Function, Low-computation, Hybrid event-triggered**

I. Introduction

THE switched nonlinear systems consist of multiple subsystems and a switching signal that determines which subsystem is active. Since switched nonlinear systems do not inherit the stability properties of subsystems, stability research for non-switched systems is not fully applicable to switched systems. Currently, various methods have been developed to analyze its stability, such as Common Lyapunov Function [1], Multiple Lyapunov Function [2], [3], and Switched Lyapunov Function [4]. In [5], [6], [7], for switched nonlinear systems with unmeasurable states, adaptive control schemes with unknown dead-zone, input saturation and fixed time control were solved respectively. However, the backstepping method employed in these studies necessitated the differentiation of virtual control signals at each step, causing the computational complexity to escalate rapidly with the order of the systems, ultimately resulting in overly complex controllers. Therefore, the contributions in the aforementioned literatures still had some limitations.

Manuscript received September 18, 2024; revised December 26, 2024. This work is supported by the Fundamental Research Funds for the Liaoning Universities of China (Grant No. LJ212410146005).

Tiantian Teng is a postgraduate student of School of Electronic and Information Engineering, University of Science and Technology Liaoning, Anshan, Liaoning, 114051, China (e-mail: 2993918235@qq.com).

Nannan Zhao is a professor of the School of Electronic and Information Engineering, University of Science and Technology Liaoning, Anshan, Liaoning, 114051, China (Corresponding author, e-mail: 723306003@qq.com).

Xinyu Ouyang is a professor of the School of Electronic and Information Engineering, University of Science and Technology Liaoning, Anshan, Liaoning, 114051, China (Corresponding author, e-mail: 13392862@qq.com).

So as to address the issue of complexity explosion, Swaroop et al. developed the Dynamic Surface Control (DSC) in [8], which incorporated dynamic filters to remove the necessity for repeatedly differentiating virtual control laws. DSC transforms the calculation of the high-order derivative of the virtual control laws into a simple algebraic operation of the filtered signal [9], [10], [11]. However, it is essential to acknowledge that the implementation of filters also results in intricate control structures and increases computational burden. [12] proposed a low-computation control method through proof by contradiction, in which the complexity explosion is avoided without utilizing DSC, meanwhile simplifying the structure of controller. Building on this foundation, this paper will introduce a low-computation adaptive control method to avoid the complexity explosion.

In practical engineering systems, such as automatic control [13], aerospace [14], and robotics [15], constraints on tracking and state errors are essential due to safety and efficiency considerations. Currently, the methods to constrain errors mainly include prescribed performance control (PPC) [16], [17] and Barrier Lyapunov Function (BLF) [18], [19]. Utilizing BLF to constrain tracking and state errors and further achieving comprehensive constraints on the system states was proposed in [20]. Inspired by it, [21] addressed the problem of full-state constraint control for pure-feedback systems by employing the mean value theorem. Notably, over-parameterization was avoided by not introducing excessive adjustable parameters. The designed controller, however, required all system states to be measurable, whereas in practical engineering, usually only the output signal is measurable. DSC based on state observers for nonlinear systems with full-state constraints was put forward in [22], refining the accuracy of control. However, this study only focused on non-switched systems. [23] considered switched systems along with average dwell time, but did not take into account saving communication resources. Unlike the aforementioned articles, the hybrid event-triggered controller designed in this paper will not only address computational limitations, but also conserve communication resources.

The computational and processing capabilities of system components are limited, as is the shared network bandwidth. Therefore, it is essential to consider whether signals can be transmitted only when necessary rather than continuously. This consequently engendered the concept of triggering [24]. [25] introduced event-triggered control, where control signals were intermittently transmitted to the actuator based on the predefined conditions. Subsequently, [26] put forward a variety of triggering mechanisms that did not require Input-to-State Stability (ISS), which improves the realizability.

Additionally, the compensation mechanism was used to deal with the event-triggered of switched nonlinear systems, effectively avoiding the problem of mismatch between switching and triggering intervals in [27].

Most current triggering mechanisms focused on the controller-to-actuator end. While this approach achieves resource savings to some extent, the transmission between sensors and the controller still occurs in the form of continuous signals, which is often unnecessary. However, when employing event-triggered to transmit state signals, the information becomes discontinuous, making virtual control signals non-differentiable, and thus rendering the backstepping inapplicable. Therefore, control strategies incorporating event-triggering mechanisms at the sensor end, i.e. state event-triggered, are relatively scarce currently. [28] considered both triggered and non-triggered cases, replacing the triggered signal with continuous output signal, under the premise of considering the errors, thus undoubtedly increasing the computational burden of the sensor. Building on [28], [29] directly considered output triggered. The first-order differentiability of the virtual control signal is ensured through designing stabilization error, while the computation of higher-order derivatives is avoided by DSC. However, although [29] reduced the computational burden on the sensors, it also introduced a relatively complex controller structure. Furthermore, the above papers did not consider hybrid event-triggered control under switched nonlinear systems, nor did they implement constraints on errors.

In conclusion, motivated by the previous studies, we propose a low-computation event-triggered control scheme for switched nonlinear systems. By employing BLFs, an errors-constrained and tracking control scheme is successfully achieved. Different from the existing papers, event-triggering mechanisms for both output and control input signals are considered, effectively conserving transmission resources. The main contribution has the following three aspects.

(1) Given that only the output signal is measurable in the design process of the controller, this paper integrates the output signal after triggering into the state observers, thereby achieving observation of the unmeasurable states. Additionally, the introduction of BLF effectively constrains the errors.

(2) In the design process, not only is the control event-triggering mechanism used in [12], [26], [27], [30], [31] considered, but output event-triggering mechanism is also taken into account. Continuous state estimates obtained through the state observers are employed to construct system errors, thereby overcoming the difficulty of state discontinuity leading to the non-existent derivative of the virtual control signal. Through the introduction of hybrid event-triggered, the data transmission and communication resource requirements are significantly reduced and the computational burden on sensors and controllers is greatly alleviated.

(3) Existing designs which apply output event-triggered, as discussed in [28] and [29], are limited to non-switched nonlinear systems, whereas this paper extends the applicability to switched systems. Meanwhile, compared with [28] and [29], we do not introduce additional filters in the design process, which simplifies the structure of the controller. Additionally, by integrating adaptive compensation terms, unnecessary triggering resulted from switching between different subsystems is eliminated.

II. System descriptions and basic knowledge

Consider the strict-feedback switched nonlinear systems as follows:

$$\begin{cases} \dot{x}_i = f_{i\sigma(t)}\left(\bar{x}_i\right) + x_{i+1} + d_{i\sigma(t)}\left(t\right), \\ \dot{x}_n = f_{n\sigma(t)}\left(\bar{x}_n\right) + u_{\sigma(t)} + d_{n\sigma(t)}\left(t\right), \\ y = x_1, \end{cases} \tag{1}$$

where $x = [x_1, x_2, \ldots, x_n]^{\mathrm{T}} \in R^n$ denotes the state vector, and only x_1 is measurable. $u_{\sigma(t)} \in R$ and $y \in R$ represent the control input and output of the system, respectively. The function $\sigma(t)$: $R_+ \to \mathbb{M} = \{1, 2, \ldots, m\}$ is a switching signal. When $\sigma(t) = k$, the kth subsystem is in a running state. $f_{ik}(\cdot)$, $i = 1, 2, \ldots, n$, $k \in \mathbb{M}$ are unknown smooth nonlinear functions. d_{ik} are external disturbances.

Assumption 1 [30]**.** There exists an unknown positive constant $\bar{f}_{ik}$ such that $|f_{ik}\left(\bar{x}_i\right)| \leq \bar{f}_{ik}$.

Assumption 2 [32]**.** The unknown disturbance is bounded, and satisfies $|d_{ik}(t)| \leq \bar{d}_{ik}$, where $\bar{d}_{ik}$ is an unknown positive constant.

Assumption 3. Only the reference signal $y_d\left(t\right)$, its first derivative $\dot{y}_d\left(t\right)$ and second derivative $\ddot{y}_d\left(t\right)$ are bounded and available.

Remark 1. Assumption 3 relaxes the requirement for prior knowledge of the systems. In articles such as [2], [7], [23], [27], the reference signal must be nth-order differentiable. However, in practical applications, obtaining high-order derivatives of the reference signal is challenging, which makes this assumption rather stringent. This paper achieves the same or even more comprehensive control objectives with less prior knowledge, thereby enhancing applicability to practical systems.

Definition 1 [12]**.** For any positive constant ι and $\chi \in \mathbb{R}$, the following inequality holds:

$$0 \leq |\iota| - \iota \tanh\left(\frac{\iota}{\chi}\right) \leq 0.2785\chi. \tag{2}$$

Definition 2 [33]**.** For $\forall T \geq t \geq 0$, let $N_{\sigma(t)}\left(T,\, t\right)$ denote the number of switches of over interval $[t,\, T)$, if there exist positive constants τ_a and N_0 such that

$$N_{\sigma(t)}(T,\, t) \leq N_0 + \frac{T - t}{\tau_a} \tag{3}$$

holds, then τ_a is called average dwell time.

III. Event-triggering mechanism

To minimize data transmission and conserve communication resources, this paper simultaneously considers hybrid event-triggering mechanisms as follows:

(1) Sensor to controller, i.e. output event-triggered

$$\begin{aligned} \check{y}_{\sigma(t)}(t) &= y_{\sigma(t_{1,J})}(t_{1,J}),\, t \in [t_{1,J},\, t_{1,J+1}), \\ t_{1,J+1} &= \inf\{t > t_{1,J} \,|\, \left|e_{y,\sigma(t)}(t)\right| \geq \eta_y\}. \end{aligned} \tag{4}$$

(2) Controller to actuator, i.e. control event-triggered

$$u_{\sigma(t)}(t) = w_{\sigma(t_J)}(t_J),\, t \in [t_J,\, t_{J+1}),$$

$$t_{J+1} = \inf\{t > t_J \,|\, \left|e_{w,\sigma(t)}(t)\right| \geq \eta_w + \upsilon_1 \left|E_J^{jst}\right|\}, \tag{5}$$

$$E_J^{jst} = \begin{cases} \omega_{\sigma(t_{s1})}(t_{s1}) - \omega_{\sigma(t_J)}(t_{s1}), & t \in [t_{s1}, \bar{t}_J), \\ 0, & otherwise, \end{cases}$$
$$\bar{t}_J = \begin{cases} t_{s2}, & N_k > 1, \\ t_{J+1}, & N_k = 1, \end{cases} \quad (6)$$

where $\left|e_{y,\sigma(t)}(t)\right| = \left|y_{\sigma(t)}(t) - \check{y}_{\sigma(t)}(t)\right|$ and $\left|e_{w,\sigma(t)}(t)\right| = \left|w_{\sigma(t)}(t) - u_{_{\sigma(t)}}(t)\right|$. $t_{1,J}$ and t_J denote the triggering time instants for sensor output and control signal, respectively. t_{s1} and t_{s2} are the switching time. E_J^{jst} represents the error caused by the different control signals between different subsystems when jth switch occurs within the triggering interval. $\bar{t}_J$ is the number of switches on (t_J, t_{J+1}). η_y, η_w, $\bar{\eta}_y > \eta_y$, $\bar{\eta}_w > \eta_w$, $\upsilon_1 \geq 1$ are positive designed constants. According to the above event-triggering mechanisms, when the measurement errors $\left|e_{y,\sigma(t)}(t)\right|$ and $\left|e_{w,\sigma(t)}(t)\right|$ exceed certain thresholds η_y and η_w, repectively, the output and control signals are transmitted.

Remark 2. During the design process, multiple subsystems are made to track the same reference signal, which implies that the output signal of each subsystem is close to the same function. As a result, the switching instants have little effect on the system states and output, in other words, at these moments, neither the states nor the output undergoes abrupt changes. Therefore, there is no need to consider that switching may cause unnecessary triggers.

IV. State observer design

For estimating the unknown states of the systems, the state observers are designed as

$$\begin{cases} \dot{\hat{x}}_i = L_{ik}(\check{y} - \hat{y}) + \hat{x}_{i+1}, \\ \dot{\hat{x}}_n = L_{nk}(\check{y} - \hat{y}) + u_k, \\ \hat{y} = \hat{x}_1, \end{cases} \quad (7)$$

where $\hat{x}_i$ is the estimation of x_i, and the estimation error $e_i = x_i - \hat{x}_i$, $i = 1, 2, \cdots, n$.

Combined with (1) and (7), one has

$$\dot{e} = A_k e + L_k(y - \check{y}) + F_k + d_k, \quad (8)$$

where $e = \begin{bmatrix} e_1 \\ e_2 \\ \vdots \\ e_n \end{bmatrix}$, $A_k = \begin{bmatrix} -L_{1k} & & & \\ -L_{2k} & & & \\ \vdots & & I_{n-1} & \\ -L_{nk} & 0 & \cdots & 0 \end{bmatrix}$, $L_k = \begin{bmatrix} L_{1k} \\ L_{2k} \\ \vdots \\ L_{nk} \end{bmatrix}$, $F_k = \begin{bmatrix} f_{1k}(x_1) \\ f_{2k}(\bar{x}_2) \\ \vdots \\ f_{nk}(\bar{x}_n) \end{bmatrix}$, $d_k = \begin{bmatrix} d_{1k} \\ d_{2k} \\ \vdots \\ d_{nk} \end{bmatrix}$.

The designed parameters L_{ik} are selected such that A_k is a Hurwitz matrix, which means for any given matrix $Q_k > 0$, there exists a matrix that holds the following equation:

$$A_k^{\mathrm{T}} P_k + P_k A_k = -Q_k. \quad (9)$$

The Lyapunov function is chosen as

$$V_{0k} = e^{\mathrm{T}} P_k e. \quad (10)$$

On the basis of (8) and (9), $\dot{V}_{0k}$ is calculated as follows:

$$\dot{V}_{0k} = -e^{\mathrm{T}} Q_k e + 2e^T P_k \left[L_k(y - \check{y}) + F_k + d_k\right]. \quad (11)$$

Referring to Young's inequality, it can be deduced that

$$2e^{\mathrm{T}} P_k L_k(y - \check{y}) \leq \|e\|^2 + \|P_k\|^2 \|L_k\|^2 \bar{\eta}_y, \quad (12)$$
$$2e^{\mathrm{T}} P_k F_k \leq \|e\|^2 + \|P_k\|^2 \sum_{i=1}^{n} \overline{f}_{ik}^2, \quad (13)$$
$$2e^{\mathrm{T}} P_k d_k \leq \|e\|^2 + \|P_k\|^2 \sum_{i=1}^{n} \overline{d}_{ik}^2. \quad (14)$$

Substituting (12) - (14) into (11) results in

$$\begin{aligned} \dot{V}_{0k} &\leq -(\lambda_{\min}(Q_k) - 3)\|e\|^2 \\ &\quad + \|P_k\|^2 \left(\sum_{i=1}^{n} \overline{f}_{ik}^2 + \sum_{i=1}^{n} \overline{d}_{ik}^2 + \|L_k\|^2 \bar{\eta}_y\right) \\ &= -\varrho_{0k}\|e\|^2 + \varpi_{0k}, \end{aligned} \quad (15)$$

where $\varrho_{0k} = \lambda_{\min}(Q_k) - 3$, $\varpi_{0k} = \|P_k\|^2 \left(\sum_{i=1}^{n} \overline{f}_{ik}^2 + \sum_{i=1}^{n} \overline{d}_{ik}^2 + \|L_k\|^2 \bar{\eta}_y\right)$.

By Assumptions 1 and 2, it can be derived that $b_{0k} > 0$. Additionally, by selecting an appropriate matrix Q_k, $a_{0k} > 0$ can be ensured. This indicates that the observation error e_i gradually decreases over time, thereby guaranteeing the asymptotic stability of the observer systems.

V. Controller design and stability analysis

The auxiliary tracking error z_1, tracking error φ_1 and state error z_i are defined as

$$z_1 = \hat{x}_1 - y_d, \quad (16)$$
$$\varphi_1 = x_1 - y_d, \quad (17)$$
$$z_i = \hat{x}_i - \alpha_{i-1,k}, \quad (18)$$

where y_d is the reference signal.

It is necessary to establish a clear definition for

$$\zeta_i = \frac{z_i}{\cos^2\left(\frac{\pi z_i^2}{2k_i^2}\right)}, \; i = 1, \cdots, n.$$

By considering the output event-triggered, the virtual control law α_{1k} and α_{ik}, $i = 2, \cdots, n$ are given as

$$\alpha_{1k} = -c_{1k}\frac{k_1^2}{\pi\zeta_1}\tan\left(\frac{\pi z_1^2}{2k_1^2}\right) - L_{1k}\bar{\eta}_y \tanh\left(\frac{\zeta_1 L_{1k}\bar{\eta}_y}{\mu}\right) + \dot{y}_d, \quad (19)$$

$$\begin{aligned} \alpha_{ik} &= -c_{ik}\frac{k_i^2}{\pi\zeta_i}\tan\left(\frac{\pi z_i^2}{2k_i^2}\right) - \frac{\zeta_{i-1}z_i}{\zeta_i} \\ &\quad - L_{ik}\bar{\eta}_y \tanh\left(\frac{\zeta_i L_{ik}\bar{\eta}_y}{\mu}\right), \end{aligned} \quad (20)$$

where c_{1k} and c_{ik} are positive constants.

Simultaneously, in the final step of backstepping, control event-triggered is implemented, where the continuous adaptive control signal w_k is expressed as

$$\begin{aligned} w_k &= -c_{nk}\frac{k_n^2}{\pi\zeta_n}\tan\left(\frac{\pi z_n^2}{2k_n^2}\right) - \frac{\zeta_{n-1}z_n}{\zeta_n} \\ &\quad - L_{nk}\bar{\eta}_y \tanh\left(\frac{\zeta_n L_{nk}\bar{\eta}_y}{\mu}\right) - L_{nk}\bar{\eta}_w \tanh\left(\frac{\zeta_n L_{nk}\bar{\eta}_w}{\mu}\right) \\ &\quad - L_{nk}\upsilon_1 E_J^{jst} \tanh\left(\frac{\zeta_n E_J^{jst}}{\mu}\right), \end{aligned} \quad (21)$$

where μ is a positive constant.

In addition, for $z_i(0)$, it satisfies $|z_i(0)| < k_i$, which is a standard assumption for dealing with constraint problems.

Remark 3. The purpose of defining the auxiliary tracking error z_1 is to ensure that the virtual control signal α_{ik} is differentiable, thereby achieving output event-triggered. In the previous section, we have demonstrated that there exists an observational error e_1 between x_1 and $\hat{x}_1$, which can be continuously minimized by selecting appropriate parameters. Moreover, through observation, the error e_1 is identified between the auxiliary tracking error z_1 and tracking error φ_1. Consequently, we can indirectly achieve tracking control and output event-triggered through auxiliary tracking error while ensuring the stability of the closed-loop systems.

Lemma 1. For each $i \in \{1, 2, \cdots, n\}$, supposed that $\dot{\hat{x}}_i$ and $z_i(t)$ are bounded, then $\dot{\alpha}_{ik}$ also remains bounded.

Proof. Taking the derivatives on both sides of (19) yields

$$\begin{aligned}\dot{\alpha}_{1k} &= c_{1k}\frac{k_1^2}{\pi}\frac{\dot{\zeta}_1}{\zeta_1^2}\tan(\frac{\pi z_1^2}{2k_1^2}) - c_{1k}\dot{z}_1 + \ddot{y}_d \\ &\quad -\dot{\zeta}_1 L_{1k}\bar{\eta}_y\left[1-\left[\tanh\left(\frac{\zeta_1 L_{1k}\bar{\eta}_y}{\mu}\right)\right]^2\right]. \quad (22)\end{aligned}$$

Derivative of both sides of (20), we have

$$\begin{aligned}\dot{\alpha}_{ik} &= c_{ik}\frac{k_i^2}{\pi}\frac{\dot{\zeta}_i}{\zeta_i^2}\tan(\frac{\pi z_i^2}{2k_i^2}) - c_{ik}\dot{z}_i \\ &\quad +\frac{\dot{\zeta}_i\zeta_{i-1}z_i}{\zeta_i^2} - \frac{\dot{\zeta}_{i-1}z_i}{\zeta_i} - \frac{\zeta_{i-1}\dot{z}_i}{\zeta_i} \\ &\quad -\dot{\zeta}_i L_{ik}\bar{\eta}_y\left[1-\left[\tanh\left(\frac{\zeta_i L_{ik}\bar{\eta}_y}{\mu}\right)\right]^2\right], \quad (23)\end{aligned}$$

where $\dot{\zeta}_i = \dot{z}_i[1+\frac{2\pi z_i^2}{k_i^2}\tan(\frac{\pi z_i^2}{2k_i^2})]\cos^{-2}(\frac{\pi z_i^2}{2k_i^2})$.

First, for $\dot{\alpha}_{1k}$, on the basic of (16) and Assumption 3, we obtain $\dot{z}_1 = \dot{\hat{x}}_1 - \dot{y}_d$ and $\dot{z}_1 \in L_\infty$. According to $z_1 \in L_\infty$, it can be obtained that $\zeta_1 \in L_\infty$ and $\dot{\zeta}_1 \in L_\infty$. Thus $\dot{\alpha}_{1k} \in L_\infty$ is deduced.

Second, for $\dot{\alpha}_{2k}$, differentiating (18) gets $\dot{z}_2 = \dot{\hat{x}}_2 - \dot{\alpha}_{1k}$. With the bound of $\dot{\alpha}_{1k}$, $\dot{z}_2 \in L_\infty$ can be achieved. Similar to the above analysis, one has ζ_2 and $\dot{\zeta}_2 \in L_\infty$. So $\dot{\alpha}_{2k} \in L_\infty$ can be obtained.

Finally, for $i = 1, 2, \cdots, n$, $\dot{\alpha}_{ik} \in L_\infty$ can be acquired recursively. Lemma 1 is proved.

Theorem 1. Suppose that the uncertain strict-feedback switched nonlinear systems (1), under given initial condition, satisfy Assumptions 1-3. If the switching signal $\sigma(t)$ satisfies $\tau_a > \frac{\ln\beta}{\varrho}$, the designed observer and controller can ensure that

(1) All variables of the closed-loop system are bounded.

(2) The tracking error and state errors can converge within a small neighborhood as $|z_i(t)| < |k_i|$.

(3) There exists a positive constant between consecutive triggers, thereby avoiding the Zeno-behavior [34].

Proof. The proof of Theorem 1 will be presented in four parts.

The boundedness of the tracking error and state errors will be demonstrated initially. A contradiction is sought by assuming the existence of z_q such that $|z_q(t_q)| \geq k_q$ at time t_q. In accordance with the initial conditions and continuity of $z_i(t)$, it can be obtained that for $t < t_m$, $t_m = \min\{t_q\}$,

$$-k_i < z_i(t) < k_i,\ i \in \{1, 2, \cdots, n\}. \quad (24)$$

Thereby, there exists z_q such that

$$\lim_{t\to t_m^-}|z_q(t)| = k_q,\ q \in \{1, 2, \cdots, n\}. \quad (25)$$

Subsequent analysis will demonstrate that the aforementioned situation does not exist.

Part (a): The tracking performance and error constraints of the systems will be demonstrated by backstepping and tangent BLFs. At the same time, output event-triggered will also be taken into account during the design process

Step 1: In view of (1) and (16), one has

$$\dot{z}_1 = z_2 + \alpha_{1k} + L_{1k}e_1 + L_{1k}(\check{y} - y) - \dot{y}_d. \quad (26)$$

The BLF on $t \in [0, t_m)$ is designed as follows:

$$V_{1k} = V_{0k} + \frac{k_1^2}{\pi}\tan(\frac{\pi z_1^2}{2k_1^2}). \quad (27)$$

Differentiating both sides of (27) results in

$$\begin{aligned}\dot{V}_{1k} &= \dot{V}_{0k} + \zeta_1[z_2 + \alpha_{1k} + L_{1k}e_1 \\ &\quad +L_{1k}(\check{y} - y) - \dot{y}_d]. \quad (28)\end{aligned}$$

With Young's inequality, it results in

$$\zeta_1 L_{1k}e_1 \leq \zeta_1^2 + \frac{1}{4}L_{1k}^2\|e\|^2.$$

Thereby, (28) can be rewritten as

$$\begin{aligned}\dot{V}_{1k} &\leq \dot{V}_{0k} - c_{1k}\frac{k_1^2}{\pi}\tan(\frac{\pi z_1^2}{2k_1^2}) + \zeta_1 z_2 \\ &\quad -\zeta_1 L_{1k}\bar{\eta}_y\tanh(\frac{\zeta_1 L_{1k}\bar{\eta}_y}{\mu}) + |\zeta_1 L_{1k}\bar{\eta}_y| + \zeta_1^2 \\ &\quad +\frac{1}{4}L_{1k}^2\|e\|^2 \\ &= \dot{V}_{0k} - c_{1k}\frac{k_1^2}{\pi}\tan(\frac{\pi z_1^2}{2k_1^2}) + \zeta_1 z_2 + 0.2785\mu + \zeta_1^2 \\ &\quad +\frac{1}{4}L_{1k}^2\|e\|^2. \quad (29)\end{aligned}$$

Step i ($i = 2, \cdots, n-1$): Based on (7) and (18), one has

$$\dot{z}_i = z_{i+1} + \alpha_{ik} + L_{ik}e_1 + L_{ik}(\check{y} - y) - \dot{\alpha}_{i-1,k}. \quad (30)$$

Construct the BLF as follows:

$$V_{ik} = V_{i-1,k} + \frac{k_i^2}{\pi}\tan(\frac{\pi z_i^2}{2k_i^2}). \quad (31)$$

Differentiating V_{ik} yields

$$\begin{aligned}\dot{V}_{ik} &= \dot{V}_{1k} + \zeta_i[z_{i+1} + \alpha_{ik} + L_{ik}e_1 \\ &\quad +L_{ik}(\check{y} - y) - \dot{\alpha}_{i-1,k}]. \quad (32)\end{aligned}$$

Through Lemma 1, we have $\dot{\alpha}_{ik} \in L_\infty$. To simplify the computational process, the partially bounded signals are defined as

$$h_{ik} = L_{ik}e_1 - \dot{\alpha}_{i-1,k} \leq \bar{h}_{ik},$$

where $\bar{h}_{ik}$ is a positive constant.

With reference to the Young's inequality, one can derive

$$\zeta_i h_{ik} \leq \zeta_i^2 + \frac{1}{4}\bar{h}_{ik}^2.$$

Then, it follows from (20) and (32) that

$$\begin{aligned}\dot{V}_{ik} &\leq \dot{V}_{1k} - c_{ik}\frac{k_i^2}{\pi}\tan(\frac{\pi z_i^2}{2k_i^2}) + \zeta_i z_{i+1} \\ &\quad -\zeta_2 L_{ik}\bar{\eta}_y \tanh(\frac{\zeta_i L_{ik}\bar{\eta}_y}{\mu}) + |\zeta_i L_{ik}\bar{\eta}_y| + \zeta_i^2 + \frac{1}{4}\bar{h}_{ik}^2 \\ &= \dot{V}_{0k} - \sum_{j=1}^{i} c_{jk}\frac{k_j^2}{\pi}\tan(\frac{\pi z_j^2}{2k_j^2}) + \sum_{j=1}^{i}\zeta_j^2 + \frac{1}{4}L_{1k}^2\|e\|^2 \\ &\quad +\frac{1}{4}\sum_{j=2}^{i}\bar{h}_{jk}^2 + \zeta_i z_{i+1} + 0.2785i\mu. \end{aligned} \tag{33}$$

Step n: On account of (7) and (18), one has

$$\dot{z}_n = u_k + L_{nk}e_1 + L_{nk}(\check{y} - y) - \dot{\alpha}_{n-1,k}. \tag{34}$$

The BLF used for the nth subsystem can be expressed as

$$V_{nk} = V_{n-1,k} + \frac{k_n^2}{\pi}\tan(\frac{\pi z_n^2}{2k_n^2}). \tag{35}$$

Then $\dot{V}_{nk}$ can be written as follows:

$$\begin{aligned}\dot{V}_{nk} &= \dot{V}_{n-1,k} + \zeta_n[u_k + L_{nk}e_1 \\ &\quad +L_{nk}(\check{y} - y) - \dot{\alpha}_{n-1,k}] \end{aligned} \tag{36}$$

Define $h_{nk} = L_{nk}e_1 - \dot{\alpha}_{n-1,k} \leq \bar{h}_{nk}$, and combined with Young's inequality again, one has

$$\zeta_n h_{nk} \leq \zeta_n^2 + \frac{1}{4}\bar{h}_{nk}^2. \tag{37}$$

Substituting (37) into (36) yields

$$\dot{V}_{nk} \leq \dot{V}_{n-1,k} + \zeta_n\left(u_k + |L_{nk}\bar{\eta}_y|\right) + \zeta_n^2 + \frac{1}{4}\bar{h}_{nk}^2, \tag{38}$$

which will be employed in the following part for the design of the event-triggered controller.

Part (b): Hybrid event-triggered adaptive controller based on control signals will be designed.

Considering that the switching instant of different subsystems in switched systems can cause sudden change in the control signal, which in turn may lead to unnecessary triggers, it is necessary to discuss the relationship between the triggering interval and switching instant during the controller design process. Therefore, it mainly includes the following three cases:

(1) the switch does not occur in the triggering interval $[t_J, t_{J+1})$;

(2) the switch appears in the triggering interval $[t_J, t_{J+1})$, including single switch and multiple switches, i.e. $t_J < t_{s1} < \cdots < t_{sj} < t_{J+1}$, $j = 1, 2, \cdots, m$;

(3) the switch occurs in the triggering instant, i.e. $t_J < t_{s1} < \cdots < t_{sj} = t_{J+1}$.

By combining with (6), the aforementioned three scenarios can be resolved by separately considering whether $E_J^{jst} = 0$.

Case 1: if $E_J^{jst} = 0$, by incorporating (5) and (21) into (38), we can conclude

$$\begin{aligned}\dot{V}_{nk,1} &\leq \dot{V}_{n-1,k} + \zeta_n\left(u_k - w_k + w_k + L_{nk}\bar{\eta}_y\right) \\ &\quad +\zeta_n^2 + \frac{1}{4}\bar{h}_{nk}^2 \\ &\leq \dot{V}_{n-1,k} + \zeta_n\left(|\bar{\eta}_w| + w_k + |L_{nk}\bar{\eta}_y|\right) + \zeta_n^2 \\ &\quad +\frac{1}{4}\bar{h}_{nk}^2 \\ &= \dot{V}_{n-1,k} - c_{nk}\frac{k_n^2}{\pi}\tan(\frac{\pi z_n^2}{2k_n^2}) - \zeta_{n-1}z_n \\ &\quad -\zeta_n L_{nk}\bar{\eta}_y\tanh(\frac{\zeta_n L_{nk}\bar{\eta}_y}{\mu}) + |\zeta_n\bar{\eta}_w| \\ &\quad -\zeta_n L_{nk}\bar{\eta}_w\tanh(\frac{\zeta_n L_{nk}\bar{\eta}_w}{\mu}) + |\zeta_n L_{nk}\bar{\eta}_y| \\ &\quad +\zeta_n^2 + \frac{1}{4}\bar{h}_{nk}^2 \\ &\leq \dot{V}_{0k} - \sum_{j=1}^{n} c_{jk}\frac{k_j^2}{\pi}\tan(\frac{\pi z_j^2}{2k_j^2}) + \sum_{j=1}^{n}\zeta_j^2 \\ &\quad +\frac{1}{4}L_{1k}^2\|e\|^2 + \frac{1}{4}\sum_{j=2}^{n}\bar{h}_{nk}^2 \\ &\quad +0.2785(n+1)\mu. \end{aligned} \tag{39}$$

Case 2: if $E_J^{jst} = w_{\sigma(t_{s1})}(t_{s1}) - w_{\sigma(t_J)}(t_{s1})$, one can deduce

$$\begin{aligned}\dot{V}_{nk,2} &\leq \dot{V}_{n-1,k} + \zeta_n\left(|\bar{\eta}_w| + \upsilon_1\left|E_J^{jst}\right| + w_k\right. \\ &\quad \left. + |L_{nk}\bar{\eta}_y|\right) + \zeta_n^2 + \frac{1}{4}\bar{h}_{nk}^2 \\ &= \dot{V}_{n-1,k} - c_{nk}\frac{k_n^2}{\pi}\tan(\frac{\pi z_n^2}{2k_n^2}) - \zeta_{n-1}z_n \\ &\quad -\zeta_n L_{nk}\bar{\eta}_y\tanh(\frac{\zeta_n L_{nk}\bar{\eta}_y}{\mu}) + |\zeta_n\bar{\eta}_w| \\ &\quad -\zeta_n L_{nk}\bar{\eta}_w\tanh(\frac{\zeta_n L_{nk}\bar{\eta}_w}{\mu}) \\ &\quad -\zeta_n\upsilon_1 E_J^{jst}\tanh(\frac{\zeta_n E_J^{jst}}{\mu}) + \upsilon_1\left|\zeta_n E_J^{jst}\right| \\ &\quad +|\zeta_n L_{nk}\bar{\eta}_y| + \zeta_n^2 + \frac{1}{4}\bar{h}_{nk}^2 \\ &\leq \dot{V}_{0k} - \sum_{j=1}^{n} c_{jk}\frac{k_j^2}{\pi}\tan(\frac{\pi z_j^2}{2k_j^2}) + \sum_{j=1}^{n}\zeta_j^2 \\ &\quad +\frac{1}{4}L_{1k}^2\|e\|^2 + \frac{1}{4}\sum_{j=2}^{n}\bar{h}_{nk}^2 \\ &\quad +0.2785(n+\upsilon_1+1)\mu. \end{aligned} \tag{40}$$

Considering (39) and (40), one has

$$\dot{V}_{nk,1} \leq \dot{V}_{nk,2} \leq -\varrho_k V_{nk} + \varpi_k, \tag{41}$$

where $\varrho_k = \min\left\{\frac{\varrho_{0k}}{\lambda_{\max}(P_k)}, c_{jk}\right\}$, $\varpi_k = \sum_{j=1}^{n}\zeta_j^2 + \frac{1}{4}L_{1k}^2\|e\|^2 + \frac{1}{4}\sum_{j=2}^{n}\bar{h}_{nk}^2 + 0.2785(n+1)\mu + \varpi_{0k}$.

Multiplying both sides of (41) by $e^{\varrho_k t}$ and integrating get

$$V_{nk} \leq (V_n(0) - \frac{\varpi_k}{\varrho_k})e^{-\varrho_k t} + \frac{\varpi_k}{\varrho_k}. \tag{42}$$

Therefore, the following inequality holds

$$V_i(t) \leq V_n(t) \leq (V_n(0) - \frac{\varpi_k}{\varrho_k})e^{-\varrho_k t} + \frac{\varpi_k}{\varrho_k}.$$

Further, combining with (27), (31), and (35), it can be obtained that

$$\begin{aligned} |z_i| &\leq |k_i| \sqrt{\frac{2}{\pi} \arctan \frac{\pi}{k_i^2} \left[(V_n(0) - \frac{\varpi_k}{\varrho_k}) e^{-\varrho_k t} + \frac{\varpi_k}{\varrho_k} \right]} \\ &< |k_i|. \end{aligned} \tag{43}$$

(43) indicates that the functions $z_1, \cdots, z_n$ remain bounded within the interval $[0, t_m)$, which contradicts (25). Thus, for any error z_i and $t < t_m$, $|z_i|$ does not approach to the constrained boundary $|k_i|$. Consequently, the proposed hypothesis (25) is invalid, and as a result, (24) holds consistently.

Remark 4. Through the above analysis, it can be concluded that the different subsystems of the switched systems are stable. However, the stability of each subsystem does not directly guarantee the global stability of the entire switched system, because the switching frequency and switching time can affect the overall behavior of the systems. Therefore, with the introduction of the average dwell time to control the switching frequency, the Lyapunov function can be reduced or maintained within a bounded range, which is crucial for ensuring the global stability of the system. Consequently, designing a suitable Lyapunov function for the whole system and conducting detailed analysis are imperative to ensure overall stability even during switches.

Part (c): The following proof will display that the overall system is stable.

Define the Lyapunov function as $V_k = V_{nk}$, according to (41), one has $\dot{V}_k \leq -\varrho V_k + \varpi$, where $\varrho = \min_{k\in\mathbb{M}}\{\varrho_k\}$, $\varpi = \max_{k\in\mathbb{M}}\{\varpi_k\}$. Define the function $W(t) = e^{\varrho t} V_{\sigma(t)}(t)$, which is piecewise differentiable along solutions of the systems. Within each interval $[t_l, t_{l+1})$, we have

$$\dot{W}(t) = \varrho e^{\varrho t} V_{\sigma(t)}(t) + e^{\varrho t} \dot{V}_{\sigma(t)}(t) \leq \varpi e^{\varrho t}. \tag{44}$$

For $\forall k,\ l \in \mathbb{M}$, $V_k(t) \leq \beta V_l(t)$ and $\beta \geq 1$ one has

$$\begin{aligned} W(t_{l+1}) &\leq \beta e^{\varrho t_{l+1}} V_{\sigma(t_l)}(x(t_{l+1})) = \beta W(t_{l+1}^-) \\ &\leq \beta \left[W(t_l) + \int_{t_l}^{t_{l+1}} \varpi e^{\varrho t} dt \right]. \end{aligned} \tag{45}$$

By selecting an arbitrary $\bar{t} > t_0 = 0$ and iterating (45) from $l = 0$ to $l = N_\sigma(\bar{t}, 0) - 1$, it can be obtained that

$$\begin{aligned} W(\bar{t}^-) &\leq W(t_{N_\sigma(\bar{t},0)}) + \int_{t_{N_\sigma(\bar{t},0)}}^{\bar{t}} \varpi e^{\varrho t} dt \\ &\leq \beta^{N_\sigma(\bar{t},0)} \left[W(0) + \sum_{l=0}^{N_\sigma(\bar{t},0)-1} \beta^{-l} \int_{t_l}^{t_{l+1}} \varpi e^{\varrho t} dt \right. \\ &\quad \left. + \beta^{-N_\sigma(\bar{t},0)} \varpi e^{\varrho t} dt \right]. \end{aligned} \tag{46}$$

Since $\tau_a > \frac{\ln\beta}{\varrho}$, for any $\delta \in (0,\ \varrho - \frac{\ln\beta}{\tau_a})$, one has $\tau_a > \frac{\ln\beta}{\varrho - \delta}$.

Based on Definition 2, it can be argued that

$$\begin{aligned} N_\sigma(\bar{t},\ t) &\leq N_0 + \frac{(\varrho - \delta)(\bar{t} - t)}{\ln\beta}, \\ N_\sigma(\bar{t},\ 0) - l &\leq 1 + N_\sigma(\bar{t},\ t_{l+1}), \\ \beta^{N_\sigma(\bar{t},0)-l} &\leq \beta^{1+N_0} e^{(\varrho-\delta)(\bar{t}-t_{l+1})}. \end{aligned} \tag{47}$$

Because of $\delta < \varrho$, it follows that

$$\int_{t_l}^{t_{l+1}} \varpi e^{\varrho t} dt \leq e^{(\varrho-\delta)t_{l+1}} \int_{t_l}^{t_{l+1}} \varpi e^{\varrho t} dt. \tag{48}$$

Substituting (47) and (48) into (46) yields

$$W(\bar{t}^-) \leq \beta^{N_\sigma(\bar{t},0)} W(0) + \beta^{1+N_0} e^{(\varrho-\delta)\bar{t}} \int_0^{\bar{t}} \varpi e^{\varrho t} dt. \tag{49}$$

It is easy to deduce that there exist two κ functions $\underline{\kappa}(|x|)$ and $\bar{\kappa}(|x|)$ such that $\underline{\kappa}(|x|) \leq V_k(x) \leq \bar{\kappa}(|x|)$ establish. Then it yields that

$$\begin{aligned} \underline{\kappa}(\|x(\bar{t})\|) &\leq V_{\sigma(\bar{t}^-)}\left(x\left(\bar{t}^-\right)\right) \\ &\leq e^{N_0 \ln\beta} e^{\left(\frac{\ln\beta}{\tau_a} - \varrho\right)\bar{t}} \bar{\kappa}(\|x(0)\|) \\ &\quad + \beta^{1+N_0} \frac{\varpi}{\delta} \left(1 - e^{-\delta\bar{t}}\right) \\ &\leq e^{N_0 \ln\beta} e^{\left(\frac{\ln\beta}{\tau_a} - \varrho\right)\bar{t}} \bar{\kappa}(\|x(0)\|) \\ &\quad + \beta^{1+N_0} \frac{\varpi}{\delta}. \end{aligned} \tag{50}$$

Therefore, given $\delta > 0$ and (50), it can be concluded that if the switching signals $\sigma(t)$ satisfies $\tau_a > \frac{\ln\beta}{\varrho}$, the whole system remains stable.

Combining with (35) and (50), the error can be obtained that

$$\begin{aligned} \lim_{t\to\infty} \frac{k_i^2}{\pi} \tan(\frac{\pi z_i^2}{2k_i^2}) &\leq e^{N_0 \ln\beta} e^{\left(\frac{\ln\beta}{\tau_a} - \varrho\right)\bar{t}} \bar{\kappa}(\|x(0)\|) \\ &\quad + \beta^{1+N_0} \frac{\varpi}{\delta}. \end{aligned}$$

Thereby, we can obtain

$$|z_i| \leq |k_i| \sqrt{\frac{2}{\pi} \arctan(\frac{\pi}{k_i^2} \beta^{1+N_0} \frac{\varpi}{\delta})}. \tag{51}$$

It can be inferred that all signals of the closed-loop systems are bounded at all times according to (51), satisfying the condition of semi-global uniform ultimate boundedness, which means that the whole system is stable under certain switching conditions.

Part (d): Given the inherent complexity of the event-triggering mechanism in switched nonlinear systems, various scenarios will be addressed separately to prevent Zeno-behavior.

Because we have adopted a dual-channel hybrid event-triggering mechanisms, it is necessary to analyze the output event-triggered from sensor to controller and the control event-triggered from controller to actuator separately to determine whether Zeno-behavior can be avoided.

A. Zeno-free of output event-triggered

In order to prove that there exists a constant $T_1 > 0$ such that $\{t_{1,J+1} - t_{1,J}\} \geq T_1$, $\forall J \in \mathbb{Z}^+$, we recall the definition of $e_{y,\sigma(t)}(t)$: $e_{y,\sigma(t)}(t) = y_{\sigma(t)}(t) - \check{y}_{\sigma(t)}(t)$. Then, we obtain

$$\begin{aligned} \frac{d}{dt} \left| e_{y,\sigma(t)}(t) \right| &= \frac{d}{dt} (e_{y,\sigma(t)}(t) * e_{y,\sigma(t)}(t))^{\frac{1}{2}} \\ &= sign(e_{y,\sigma(t)}(t)) \dot{y}_{\sigma(t)}(t) \\ &\leq \left| \dot{y}_{\sigma(t)}(t) \right|. \end{aligned} \tag{52}$$

Since $\dot{y}_{\sigma(t)}(t)$ is bounded, hence, there must exist a constant $s_{y,E} > 0$ such that $\left|\dot{y}_{\sigma(t)}(t)\right| < s_{y,E}$. So it yields

$$\begin{aligned} \dot{e}_{y,\sigma(t)}(t) &= \frac{\eta_y}{t_{J+1} - t_J} \leq s_{y,E}, \\ t_{J+1} - t_J &\geq \frac{\eta_y}{s_{y,E}} = T_1. \end{aligned} \tag{53}$$

The Zeno-behavior is therefore avoided successful.

B. Zeno-free of control event-triggered

Considering that the switching moment between different subsystems of the switched systems may affect the control signal, and then affect the triggering mechanism, three situations need to be analyzed.

Case 1: When there is no switch in the triggering interval $[t_J,\, t_{J+1})$ or the switch takes place exactly at the triggering instant, then for $t = t_{J+1}$ the measurement error $\left|e_{\sigma(t)}\left(t\right)\right| \geq \eta_w$. Therefore, it can be derived that

$$\begin{aligned}\frac{d}{dt}\left|e_{w,\sigma(t)}\left(t\right)\right| &= \frac{d}{dt}(e_{w,\sigma(t)}\left(t\right) * e_{w,\sigma(t)}\left(t\right))^{\frac{1}{2}} \\ &= sign(e_{w,\sigma(t)}\left(t\right))\dot{e}_{w,\sigma(t)}\left(t\right) \\ &\leq \left|\dot{e}_{w,\sigma(t)}\left(t\right)\right| = \left|\dot{\omega}_{\sigma(t)}\left(t\right)\right| \\ &\leq \left|\frac{d}{dt}\left[-c_{nk}\frac{k_n^2}{\pi\zeta_n}\tan(\frac{\pi z_n^2}{2k_n^2})\right.\right. \\ &\quad -\frac{\zeta_{n-1}z_n}{\zeta_n} - L_{nk}\bar{\eta}_y\tanh(\frac{\zeta_n L_{nk}\bar{\eta}_y}{\mu}) \\ &\quad \left.\left.-L_{nk}\bar{\eta}_w\tanh(\frac{\zeta_n L_{nk}\bar{\eta}_w}{\mu})\right]\right|. \qquad (54)\end{aligned}$$

The boundedness of all signals has been proved in the previous parts, hence, there must exist a positive constant $s_{w,E}$ satisfying $\left|\dot{\omega}_{\sigma(t)}\left(t\right)\right| \leq s_{w,E}$.

$$\dot{e}_{w,\sigma(t)}\left(t\right) = \frac{\eta_w}{t_{J+1}-t_J} \leq s_{w,E},$$

$$t_{J+1} - t_J \geq \frac{\eta_w}{s_{w,E}} = T_2. \qquad (55)$$

Case 2: When the subsystem is switched (one switch) within the triggering interval time $[t_J,\, t_{J+1})$, i.e. $t_{s1} \in [t_J,\, t_{J+1})$. The whole interval is divided into three cells for analysis:

(1) Within the time interval $[t_J,\, t_{s1})$, the analysis is the same as in Case 1.

(2) Within the time interval $[t_{s1}^-,\, t_{s1}^+]$, one has $\left|w_{\sigma(t_J)}(t_J) - w_{\sigma(t_J)}(t_{s1})\right| < \eta_w + \nu_1\left|E_J^{jst}\right|$, and

$$\begin{aligned}\left|e_{w,\sigma(t_{s1})}\left(t_{s1}\right)\right| &= \left|\omega_{\sigma(t_J)}\left(t_J\right) - \omega_{\sigma(t_{s1})}\left(t_{s1}\right)\right| \\ &\leq \left|\omega_{\sigma(t_J)}\left(t_J\right) - \omega_{\sigma(t_J)}\left(t_{s1}\right)\right| \\ &\quad + \left|\omega_{\sigma(t_J)}\left(t_{s1}\right) - \omega_{\sigma(t_{s1})}\left(t_{s1}\right)\right| \\ &< \eta_w + \nu_1\left|E_J^{jst}\right|,\end{aligned}$$

which implies that the triggering condition is not satisfied at t_{s1}.

(3) Within the time interval $(t_{s1},\, t_{J+1})$, we have

$$\frac{d}{dt}\left|e_{w,\sigma(t)}\left(t\right)\right| \leq \left|\dot{e}_{w,\sigma(t)}\left(t\right)\right| = \left|\dot{\omega}_{\sigma(t)}\left(t\right)\right|,$$

$$\dot{e}_{w,\sigma(t)}\left(t\right) = \frac{\eta_w + \nu_1\left|E_J^{jst}\right|}{t_{J+1}-t_J} \leq s_{w,E}^*.$$

Consequently, it can be inferred that $t_{s1} - t_J \geq \frac{\eta_w}{s_{w,E}} = T_2$ and $t_{J+1} - t_{s1} \geq \frac{\eta_w + \nu_1\left|E_J^{jst}\right|}{s_{w,E}^*} \geq \frac{\eta_w}{s_{w,E}^*} = T_2^*$.

The combination of these two expressions yields

$$t_{J+1} - t_J \geq \frac{\eta_w}{\max\{s_{w,E},\, s_{w,E}^*\}} = \min\{T_2,\, T_2^*\}. \qquad (56)$$

Case 3: Multiple switches occur during the triggering interval $[t_J,\, t_{J+1})$. And we have

$$t_{J+1} - t_J \geq N\tau_a.$$

Above all, the analysis of Cases 1-3 demonstrates that for any bounded condition, the control event-triggering mechanism (5) and (6) has a positive minimum triggering time t^*, and

$$t^* = \min\left\{\min\{T_2,\, T_2^*\},\, \tau_a\right\}. \qquad (57)$$

So far, Zeno-behavior has been successfully avoided.

Remark 5. The low-computation mentioned in this paper is mainly reflected in two aspects:

(1) In contrast to [28], this paper does not choose to trigger the virtual control signal simultaneously with the output signal. Instead, we obtain a continuous estimate of the system states by constructing suitable state observers and selecting the error $z_1 = \hat{x}_1 - y_d$ rather than $z_1 = x_1 - y_d$. The virtual control law is then constructed using the continuous signal $z_i,\, i = 1,\, 2,\, \cdots,\, n$ to be derivable. Therefore, the computing burden of the sensor is reduced.

(2) However, the higher-order derivative of virtual control signal does not exist when applying the same backstepping as in [2], [26], [27]. Therefore, in this paper, a new low-computation method is employed, in which the boundedness of the virtual control law is assessed and scaled, so as to avoid the presence of higher-order derivative and complete the stability analysis of the systems. Additionally, unlike [23], [29], the avoidance of higher-order derivative is not achieved through DSC, nor are additional filters introduced in this paper, resulting in a relatively simpler control signal, thereby reducing the computational burden and design complexity.

As a result, the discontinuity of the signal caused by output event-triggered is successfully overcome in this paper, and the computational and transmission burdens are reduced.

VI. Simulation

A second-order switched nonlinear system is considered as follows:

$$\begin{cases}\dot{x}_1 = f_{1k}(x_1) + x_2 + d_{1k}, \\ \dot{x}_2 = f_{2k}(\bar{x}_2) + u_k + d_{2k}, \\ y = x_1.\end{cases} \qquad (58)$$

When $k = 1$, $f_{1,1} = 0.1\sin(x_1^2)$, $f_{2,1} = 0.2\sin(x_1x_2)$, $d_{1,1} = 0.02\cos(t)$, $d_{2,1} = 0.01\sin(t)$. When $k = 2$, $f_{2,1} = 0.15x_1$, $f_{2,1} = 0.1x_1x_2$, $d_{2,1} = 0.05\sin(t)$, $d_{2,2} = 0.02\cos(t)$. The reference signal y_d is given as $y_d = 0.25\sin(t)$.

The initial conditions selected in the simulation are $[x_1(0),\, x_2(0)]^{\mathrm{T}} = [0.05,\, 0]^{\mathrm{T}}$, $[\hat{x}_1(0),\, \hat{x}_2(0)]^{\mathrm{T}} = [0.05,\, 0.05]^{\mathrm{T}}$. The parameters are selected as $L_{11} = 1$, $L_{12} = 2$, $L_{21} = 7$, $L_{22} = 5$, $c_{11} = 10$, $c_{12} = 15$, $c_{21} = 1$, $c_{22} = 2$, $k_1 = 0.08$, $k_2 = 0.1$, $\eta_y = 0.08$, $\bar{\eta}_y = 0.1$, $\eta_w = 0.5$, $\bar{\eta}_w = 0.6$, $\mu = 2$, $\upsilon_1 = 1.2$. The average dwell time is chosen as $\tau_a = 7.5$.

The simulation time is set to $80s$. Figs. 1-8 illustrate the simulation results of the designed control strategy. The continuous output signal $y(t)$ and the output event-triggered signal $\breve{y}(t)$ are presented in Fig. 4. More specifically, the number of event-triggered is 228. The continuous control input signal $\omega(t)$ and the event-triggered control signal $u(t)$,

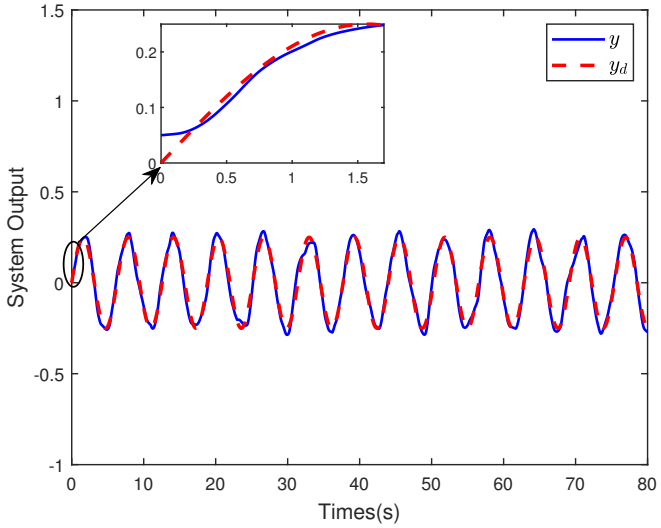

Fig. 1. The output signal y and the reference signal y_d.

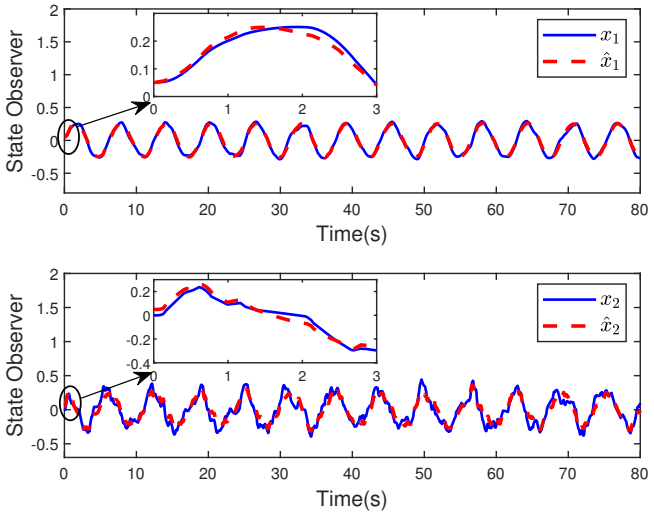

Fig. 2. The system states x_1, x_2 and their estimations $\hat{x}_1$, $\hat{x}_2$.

TABLE I
THE COMPARISON RESULTS ON THE NUMBER OF TRIGGERING-EVENTS.

Different strategies	Output event-triggered	Control event-triggered
The proposed method	228	213
The method in [27]	4000	82
The method with DSC	248	175
The method in [29]	250	548
The method with time-triggered	4000	4000

which is triggered 213 times, are shown in Fig. 5. The moments when the sensor output and control signals are triggered for $20s$ are displayed in Fig. 6.

Additionally, to further elucidate the distinctions among the existing methods, comparative simulations are performed, with the results presented in Figs. 8-9. If DSC is utilized, the resulting expression of the continuous control signal is as follows:

$$\begin{aligned} w_k \quad = \quad & -c_{nk}\frac{k_n^2}{\pi\zeta_n}\tan(\frac{\pi z_n^2}{2k_n^2}) - \frac{\zeta_{n-1}z_n}{\zeta_n} \\ & -L_{nk}\bar{\eta}_y\tanh(\frac{\zeta_n L_{nk}\bar{\eta}_y}{\mu}) - L_{nk}\bar{\eta}_w\tanh(\frac{\zeta_n L_{nk}\bar{\eta}_w}{\mu}) \\ & +\dot{\alpha}^c_{n-1,k} - L_{nk}\upsilon_1 E_J^{jst}\tanh(\frac{\zeta_n E_J^{jst}}{\mu}), \end{aligned} \tag{59}$$

where $\alpha^c_{n-1,k}$ is obtained by passing $\alpha_{n-1,k}$ through the output of a first-order low-pass filter $\vartheta_{n-1,k}\dot{\alpha}^c_{n-1,k} + \alpha^c_{n-1,k} = \alpha_{n-1,k}$, where $\vartheta_{n-1} > 0$ is the time constant. $\alpha^c_{n-1,k}(0) = \alpha_{n-1,k}(0)$ and $\alpha_{n-1,k}$ is the virtual control law. It can be observed that the proposed low-computation hybrid event-trigger adaptive control scheme has the same control effect, but further simplifies the controller structure.

With the simulation time set to $80s$, the comparison of the communication counts among the presented method, the method in [27], the method with DSC, the method in [29] and the method with time-triggered are illustrated in TABLE I. The triggering interval for time-triggered is set to $0.02s$. In contrast, the hybrid event-triggered control scheme proposed in this paper significantly conserves communication resources while achieving equivalent control performance.

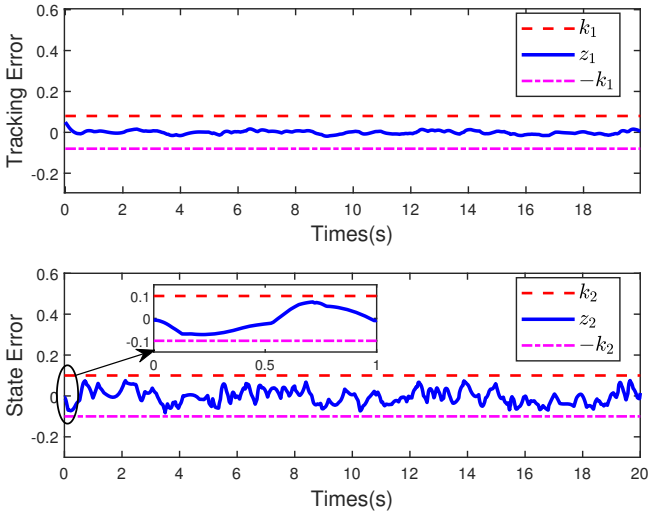

Fig. 3. The tracking error z_1 and the state error z_2.

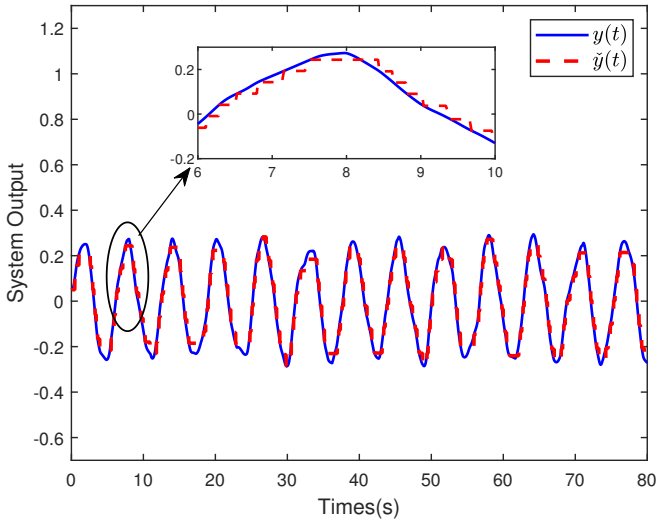

Fig. 4. Continuous output signal $y(t)$ and triggered output signal $\check{y}(t)$.

VII. CONCLUSION

A hybrid event-triggered low-computation control scheme is proposed for a family of switched nonlinear systems with

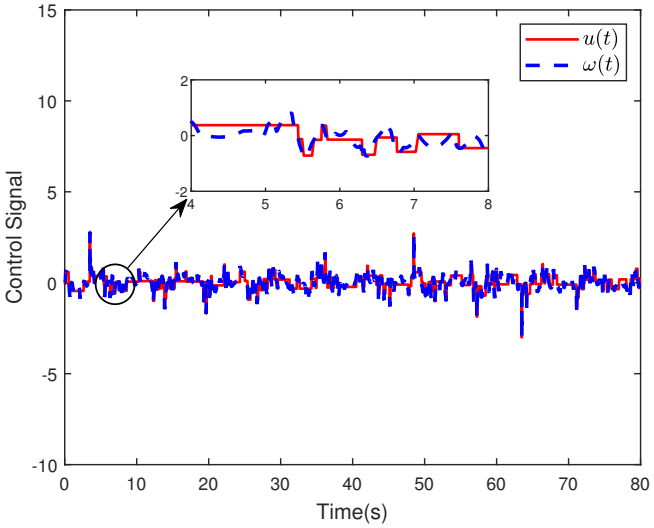

Fig. 5. Triggered control signal $u(t)$ and continuous input signal $\omega(t)$.

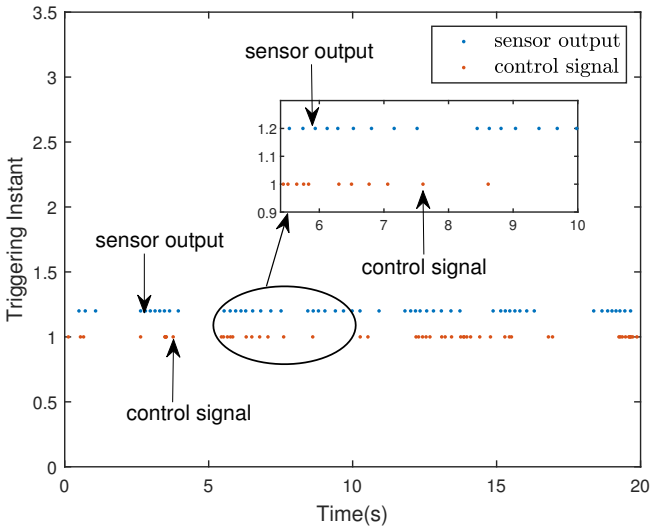

Fig. 6. Hybrid event-triggered instant.

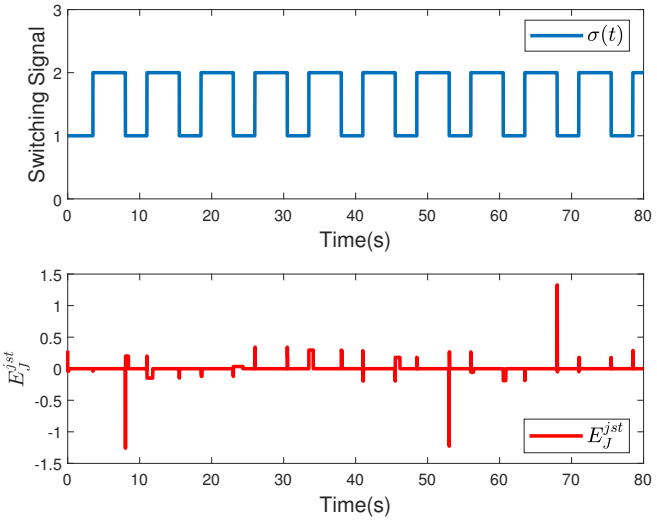

Fig. 7. The trajectories of the switching signal and E_J^{jst}.

unmeasurable states. By adopting event-triggering mechanisms in both the sensor-to-controller and controller-to-actuator channels, the communication burden is significantly

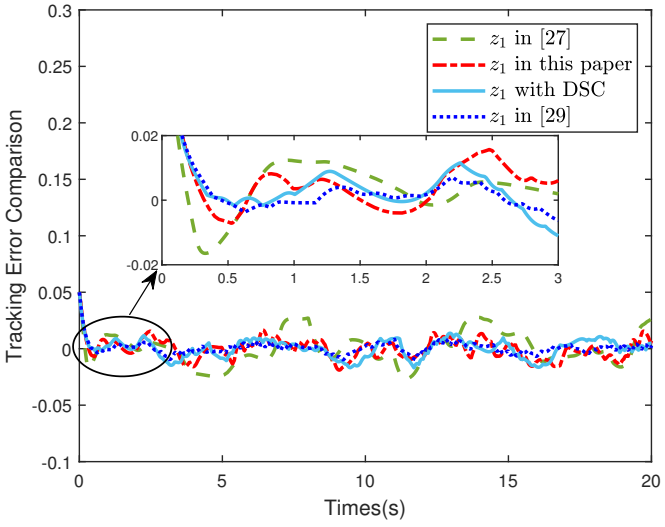

Fig. 8. The comparison results on the tracking error z_1.

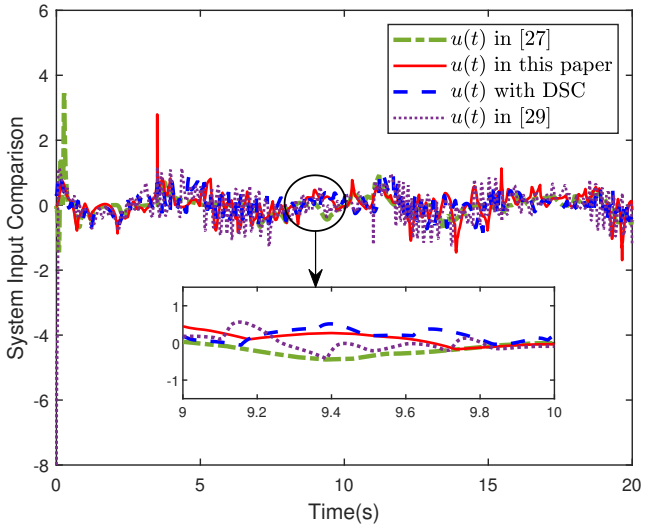

Fig. 9. The comparison results on the input signal $u(t)$.

alleviated, thereby conserving network resources. Moreover, the state observers, composed of the output signal after triggering and the measurable signal, address the problem of unmeasurable states. At the same time, by combining the stabilization errors with the observation results, the challenge of non-differentiable virtual control laws caused by triggering is successfully overcome. Additionally, the adaptive compensation term resolves the mismatch between switching and triggering intervals, and it is rigorously proven that the Zeno-behavior is absent. The applicability of the proposed output-triggered control method to MIMO nonlinear systems will be considered in future work.

REFERENCES

[1] L. Vu and D. Liberzon, "Common Lyapunov Functions for Families of Commuting Nonlinear Systems," *Systems & Control Letters*, vol. 54, no. 5, pp. 405-416, 2005.

[2] L. Long and J. Zhao, "Adaptive Output-Feedback Neural Control of Switched Uncertain Nonlinear Systems with Average Dwell Time," *IEEE Transactions on Neural Networks and Learning Systems*, vol. 26, no. 7, pp. 1350–1362, 2014.

[3] I. Tabbi, D. Jabri, I. Chekakta and D. E. C. Belkhiat, "Robust State and Sensor Fault Estimation for Switched Nonlinear Systems Based on Asynchronous Switched Fuzzy Observers," *International Journal of Adaptive Control and Signal Processing*, vol. 38, no. 1, pp. 90–120, 2024.

[4] J. Daafouz, G. Millerioux and C. Iung, "A Poly-Quadratic Stability Based Approach for Linear Switched Systems," *International Journal of Control*, vol. 75, no. 16-17, pp. 1302–1310, 2002.

[5] S. Tong, S. Sui and Y. Li, "Observed-Based Adaptive Fuzzy Tracking Control for Switched Nonlinear Systems with Dead-Zone," *IEEE Transactions on Cybernetics*, vol. 45, no. 12, pp. 2816–2826, 2015.

[6] S. Tong, Y. Li and S. Sui, "Adaptive Fuzzy Output Feedback Control for Switched Nonstrict-Feedback Nonlinear Systems with Input Nonlinearities," *IEEE Transactions on Fuzzy Systems*, vol. 24, no. 6, pp. 1426–1440, 2016.

[7] J. Zhao, X. Ouyang and N. Zhao, "Fixed-Time Adaptive Fuzzy Control of Switching Nonlinear System with Time-Varying Full-State Constraint," *Control Engineering of China*, pp. 1–10, 2023.

[8] D. Swaroop, J. K. Hedrick, P. P. Yip and J. C. Gerdes, "Dynamic Surface Control for a Class of Nonlinear Systems," *IEEE Transactions on Automatic Control*, vol. 45, no. 10, pp. 1893–1899, 2000.

[9] Z. Peng, D. Wang and J. Wang, "Predictor-Based Neural Dynamic Surface Control for Uncertain Nonlinear Systems in Strict-Feedback Form," *IEEE Transactions on Neural Networks and Learning Systems*, vol. 28, no. 9, pp. 2156–2167, 2016.

[10] D. Wang and J. Huang, "Neural Network-Based Adaptive Dynamic Surface Control for a Class of Uncertain Nonlinear Systems in Strict-Feedback Form," *IEEE Transactions on Neural Networks*, vol. 16, no. 1, pp. 195–202, 2005.

[11] L. Long and J. Zhao, "Adaptive Fuzzy Output-Feedback Dynamic Surface Control of MIMO Switched Nonlinear Systems with Unknown Gain Signs," *Fuzzy Sets and Systems*, vol. 302, pp. 27–51, 2016.

[12] D. Zhao, X. Ouyang, N. Zhao and F. Zhang, "Event-Triggered Low-Computation Adaptive Output-Feedback Fuzzy Tracking Control of Uncertain Nonlinear Systems," *ISA Transactions*, vol. 144, pp. 86–95, 2024.

[13] S. Sui, C. P. Chen and S. Tong, "A Novel Full Errors Fixed-Time Control for Constraint Nonlinear Systems," *IEEE Transactions on Automatic Control*, vol. 68, no. 4, pp. 2568–2575, 2022.

[14] P. Masarati, M. Morandini and A. Fumagalli, "Control Constraint of Underactuated Aerospace Systems," *Journal of Computational and Nonlinear Dynamics*, vol. 9, no. 2, p. 021014, 2014.

[15] Y. Wu, R. Huang, X. Li and S. Liu, "Adaptive Neural Network Control of Uncertain Robotic Manipulators with External Disturbance and Time-Varying Output Constraints," *Neurocomputing*, vol. 323, pp. 108–116, 2019.

[16] X. Bu, "Prescribed Performance Control Approaches, Applications and Challenges: A Comprehensive Survey," *Asian Journal of Control*, vol. 25, no. 1, pp. 241-261, 2023.

[17] Y. Zhou, X. Ouyang, N. Zhao, H. Xu and H. Li, "Prescribed Performance Adaptive Neural Network Tracking Control of Strict-Feedback Nonlinear Systems with Nonsymmetric Dead-Zone," *IAENG International Journal of Applied Mathematics*, vol. 51, no. 3, pp. 444-452, 2021.

[18] J. Zhang and G. Yang, "Robust Adaptive Fault-Tolerant Control for a Class of Unknown Nonlinear Systems," *IEEE Transactions on Industrial Electronics*, vol. 64, no. 1, pp. 585–594, 2017.

[19] Z. Xie, X. Chen and X. Wu, "Fixed Time Control of Free-Flying Space Robotic Manipulator with Full State Constraints: A Barrier-Lyapunov-Function Term Free Approach," *Nonlinear Dynamics*, vol. 112, no. 3, pp. 1883-1915, 2024.

[20] K. P. Tee, S. S. Ge and E. H. Tay, "Barrier Lyapunov Functions for the Control of Output-Constrained Nonlinear Systems," *Automatica*, vol. 45, no. 4, pp. 918–927, 2009.

[21] Y. Liu and S. Tong, "Barrier Lyapunov Functions-Based Adaptive Control for a Class of Nonlinear Pure-Feedback Systems with Full State Constraints," *Automatica*, vol. 64, pp. 70–75, 2016.

[22] Q. Su and M. Wan, "Adaptive Neural Dynamic Surface Output Feedback Control for Nonlinear Full States Constrained Systems," *IEEE Access*, vol. 8, pp. 131590–131600, 2020.

[23] M. Wan, S. Yang, S. Huang and D. Qizhi, "Adaptive Neural Network Control for Switched Systems with Full State Constraints," *Aerospace Control and Application*, vol. 49, no. 1, pp. 40–52, 2023.

[24] W. He, S. Li and Z. Xiang, "Research Status and Progress in Sampled-Data Control for Switched Nonlinear Systems," *Information and Control*, vol. 49, no. 2, pp. 129–138, 2020.

[25] R. Ostoyan, P. Tabuada, D. Nesic and A. Anta, "A Framework for the Event-Triggered Stabilization of Nonlinear Systems," *IEEE Transactions on Automatic Control*, vol. 60, no. 4, pp. 982-996, 2015.

[26] L. Xing, C. Wen, Z. Liu, H. Su and J. Cai, "Event-Triggered Adaptive Control for a Class of Uncertain Nonlinear Systems," *IEEE Transactions on Automatic Control*, vol. 62, no. 4, pp. 2071–2076, 2016.

[27] J. Lian and C. Li, "Event-Triggered Control for a Class of Switched Uncertain Nonlinear Systems," *Systems & Control Letters*, vol. 135, p. 104592, 2020.

[28] Z. Zhang, C. Wen, L. Xing and Y. Song, "Adaptive Event-Triggered Control of Uncertain Nonlinear Systems Using Intermittent Output Only," *IEEE Transactions on Automatic Control*, vol. 67, no. 8, pp. 4218–4225, 2021.

[29] Z. Zhang, C. Wen, L. Xing and Y. Song, "Event-Triggered Adaptive Control for a Class of Nonlinear Systems with Mismatched Uncertainties via Intermittent and Faulty Output Feedback," *IEEE Transactions on Automatic Control*, vol. 68, no. 12, pp.8142–8149, 2023.

[30] N. Zhao, X. Ouyang, L. Wu and F. Shi, "Event-Triggered Adaptive Prescribed Performance Control of Uncertain Nonlinear Systems with Unknown Control Directions," *ISA Transactions*, vol. 108, pp. 121–130, 2021.

[31] Z. Xu, C. Gao and H. Jiang, "High-Gain-Observer-Based Output Feedback Adaptive Controller Design with Command Filter and Event-Triggered Strategy," *IAENG International Journal of Applied Mathematics*, vol. 53, no. 2, pp. 463-469, 2023.

[32] L. Liu, A. Chen and Y. Liu, "Adaptive Fuzzy Output-Feedback Control for Switched Uncertain Nonlinear Systems with Full-State Constraints," *IEEE Transactions on Cybernetics*, vol. 52, no. 8, pp. 7340–7351, 2021.

[33] X. Zhao, L. Zhang, P. Shi and M. Liu, "Stability and Stabilization of Switched Linear Systems with Mode-Dependent Average Dwell Time," *IEEE Transactions on Automatic Control*, vol. 57, no. 7, pp. 1809–1815, 2011.

[34] M. Deng, Y. Dong and M. Ding, "Event-Triggered Finite-Time Stabilization of a Class of Uncertain Nonlinear Switched Systems with Delay," *IAENG International Journal of Applied Mathematics*, vol. 51, no. 3, pp. 743-750, 2021.